Nucleotide sequence context influences HIV replication fidelity by modulating reverse transcriptase binding and product release

Rio Yamanaka, John Termini*

Division of Molecular Biology, Beckman Research Institute of the City of Hope Cancer Center, Duarte, CA, USA.

SUMMARY **An RNA template/DNA primer (T/P) complex derived from the env gene of HIV-1 was used to examine the kinetic effects of specific basepair substitutions on dNTP incorporation and RNase H cleavage by HIV-1 reverse transcriptase (RT). Single basepair substitutions 2 or 6 nucleotides upstream from a defined polymerization site (denoted -2 and -6) were engineered by oligonucleotide synthesis to provide 7 T/P substrates for kinetic analysis. A -6 A/T substitution in the wild type sequence resulted in 14- and 7-fold increases in the apparent second order rate constants (k_{2app}) for U/A and U/G basepair formation. The k_{2app} for U/A formation was relatively unchanged for all other T/P basepair changes. The -6A/T substitution also uniquely lowered the RNase H cleavage rate by 3-fold. Combined kinetic and thermodynamic analyses indicated that these effects were due almost exclusively to increases in the K_D (k_{off}/k_{on}) of initial binding of RT to the T/P and the rate of product release. The data suggest that certain sequence contexts may influence RT fidelity by modulating enzyme binding/dissociation rather than by altering dNTP binding affinity or the rate of the bond forming step.**

Key Words: Reverse transcriptase, polymerase, RNase H, sequence context, steady and pre-steady state kinetics

Introduction

The relatively low fidelity of HIV-1 RT (~1 in 10^4 errors/replication cycle (*1-4*); coupled to rapid viral turnover (~10^{10} virions/day (*5*); contributes to the phenomenon of retroviral hypermutagenesis. This results in the evolution of drug resistance and escape from immune system surveillance, persistent obstacles in the treatment of AIDS. Other biochemical factors that influence HIV replication fidelity include the effects of sequence context (*6,7*), RNA secondary structure (*8,9*), accessory proteins (*10-12*) and the presence of modified bases in the RNA template and dNTP precursor pool (*13-15*). In particular, the sequence composition of the T/P stem alone appears to exert large effects on the processivity and fidelity of HIV-1 RT. For example, polymerase termination frequency can be influenced by single base substitutions upstream of the dNTP incorporation site (*6,7*). The incorporation efficiency of nucleoside analog inhibitors of RT has also been shown to be highly dependent on T/P base composition (*16*). These "indirect effects" resulting from perturbation of RT-T/P points of contact remote from the polymerization and RNase H sites can have important consequences for HIV-1 RT fidelity (*17*), but the biochemical mechanisms are poorly understood. Crystallographic studies of HIV-1 RT bound to either DNA/DNA (*18,19*) or RNA/DNA (*20*) reveal van der Waals and hydrogen bonded contacts to the T/P stem upstream of the polymerization site by residues of the palm and thumb subdomains of the p66 subunit of HIV-1 RT. Mutagenesis of these residues can result in significant modifications to the polymerase, strand transfer and RNase H activities (*21-23*), suggesting that specific interactions between amino acid side chains of HIV-1 RT and the T/P can regulate different enzymatic functions of RT.

**Correspondence to:* Division of Molecular Biology, Beckman Research Institute of the City of Hope Cancer Center, 1500 East Duarte Road, Duarte, CA 91010, USA; e-mail: jtermini@coh.org

Received June 6, 2007
Accepted June 25, 2007

We have taken a complementary approach to protein mutagenesis studies by varying single T/P basepairs predicted to be in close contact with the p66 palm and thumb subdomains of HIV-1 RT and measuring the resulting effects on dNTP incorporation and RNase H cleavage kinetics. We used an RNA template corresponding to nucleotides 962 to 996 of the *env* gene from HIV-1 clone WMJ1 (*24*) as a model sequence to examine these effects. Base substitutions were made at the -2 and -6 positions in the T/P by synthesis of the appropriate oligoribonucleotide templates and complementary DNA primers, and the corresponding effects on HIV-1 RT activity was measured using steady and pre-steady state kinetic models. Previous work using M13 DNA templates showed that the sequence composition at these positions exerted a significant effect on the termination of cDNA synthesis by HIV-1 RT (*7*), suggesting a potential role in modulating polymerase fidelity.

Materials and Methods

Oligonucleotides

RNA templates were synthesized by Dharmacon Research (Lafayette, CO, USA). RNA oligomers were deprotected according to the directions of the manufacturer and were used without further purification. DNA primers were purchased from Integrated DNA Technologies (Coralville, IA, USA). Deoxynucleoside triphosphates were purchased from Roche (Pleasanton, CA, USA). DNA oligomers were purified by 20% polyacrylamide gel electrophoresis (PAGE) and isolated using an ELUTRAP (Schleicher & Schuell BioSciences, Keene, NH, USA). DNA oligomers were desalted on Centri Spin 10 gel filtration columns (Princeton Separations, Adelphia, NJ, USA). RNA and DNA concentrations were determined spectrophotometrically using the absorbance at 260 nm according to the method of Borer (*25*). DNA primers (6 μM) were 5'-end-labeled with 10 μCi [γ-^{32}P] ATP (ICN Biomedicals, Irvine, CA, USA) and T4 polynucleotide kinase (New England Biolabs, Beverly, MA, USA) using a standard procedure. Template/primer complexes were formed by mixing RNA with a 1.5 fold excess of the corresponding DNA primer in 50 mM Tris-HCl/NaCl (pH 7.5) for 3 min at 90ºC followed by cooling over 90 min in a heat block.

Purification of HIV-1 RT

HIV-1 RT was expressed from plasmid pHIV-RT (His) Prot transformed into *E.coli* BL21 (DE3) pLysS cells (Novagen, Madison, WI, USA) and purified essentially as described (*14*) with several minor changes. The cell-free extract obtained from a 6 L culture was applied to a pre-equilibrated Ni-NTA superflow affinity column (Qiagen, Valencia, CA, USA) in metal affinity equilibration buffer (50 mM NaH_2PO_4, 300 mM NaCl, pH 7.0) at a flow rate of 0.6 mL/min using an FPLC (LCC-500 Plus, Amersham Pharmacia Biotech, Piscataway, NJ, USA). The column was washed with buffer A (50 mM NaH_2PO_4, 300 mM NaCl, 10 mM imidazole, 10% glycerol, pH 7.0) at a flow rate of 0.3 mL/min until the A_{280} was reduced to < 0.08 a.u. HIV-1 RT was eluted from the column using a gradient (10-250 mM imidazole in buffer A) at a flow rate of 0.75 mL/min. Fractions were analyzed for protein content using the Bradford reagent (Biorad, Hercules, CA, USA) and by SDS-PAGE with Coomassie staining. Fractions containing HIV-1 RT p66/p51 heterodimer were combined and concentrated using Centricon plus-20 tubes (Millipore Corporation, Bedford, MA, USA) prior to loading onto a gel filtration column (HiPrep 26/60 Sephacryl S-300; Amersham Pharmacia Biotech, Piscataway, NJ, USA) in 50 mM Tris-HCl, pH 8.0 at a flow rate of 0.8 mL/min. Aliquots determined to contain HIV-1 RT were pooled and concentrated, and enzyme concentrations were determined spectrophotometrically as previously described (*14*). The fraction of catalytically active polymerase molecules was assessed by active site titration as described below.

Steady state kinetics

HIV-1 RT (56.5 nM) was added to T/P complexes (150 nM) containing 0.1 μCi 5'γ-^{32}P end-labeled primers in 4 μL 50 mM Tris-HCl/NaCl (pH 7.5). Reactions were initiated by adding 4 μL of dATP (0.005, 0.01, 0.02, 0.05, 0.1, and 0.2 μM) or dGTP (0.025, 0.05, 0.1, 0.2, 0.4, and 0.8 mM) containing 10 mM Mg^{2+} at 37°C. Polymerization was quenched within the linear phase (30 sec and 3 min respectively for reactions with dATP and dGTP) with 16 μL of 90% formamide, 50 mM EDTA (pH 8.0), 0.1% xylene cyanol, and 0.1% bromophenol blue. Primer extension products were separated using 20% PAGE and the data were quantified by PhosphorImager analysis using the ImageQuant software package (Molecular Dynamics, Sunnyvale, CA, USA). Reaction velocity was plotted against dNTP concentration and steady state kinetic constants were determined by fitting the data to the Michaelis-Menten equation using Prism (Graph Pad Software, Inc., San Diego, CA, USA). Steady state parameters are compiled in Table 1.

Pre-steady state kinetics

Pre-steady state and active site titration experiments were carried out using a KinTek RQF3 rapid quench flow instrument (KinTek Corporation, Austin, TX, USA). Solution A, consisting of HIV-1 RT (74 nM) and T/P (30 nM) in 50 mM Tris-HCl/NaCl (pH 7.5); and Solution B, consisting of various concentrations

Table 1. Steady-state kinetic parameters

Template	Incorporation of dATP				Incorporation of dGTP			
	V_{max} (nM s^{-1})	k_{cat} (s^{-1})	K_M (μM)	k_{2app} (s^{-1} μM^{-1})	V_{max} (nM s^{-1})	k_{cat} (s^{-1})	K_M (μM)	k_{2app} ($\times 10^5$) (s^{-1} μM^{-1})
Control (WMJ1)	1.80 ± 0.05	0.0318 ± 0.0007	0.108 ± 0.006	0.30	0.33 ± 0.04	0.0059 ± 0.0007	200 ± 56	3.0
-6U/A	0.42 ± 0.01	0.0074 ± 0.0002	0.025 ± 0.002	0.29	0.082 ± 0.004	0.0015 ± 0.00007	190 ± 25	0.78
-6A/T	3.68 ± 0.06	0.0651 ± 0.0011	0.015 ± 0.001	4.3	0.625 ± 0.0098	0.0110 ± 0.0002	52 ± 3.2	21
-6G/C	0.75 ± 0.03	0.013 ± 0.0005	0.022 ± 0.003	0.59	0.256 ± 0.002	0.00452 ± 0.00004	50 ± 1.7	9.1
-2U/A	1.16 ± 0.01	0.0205 ± 0.0004	0.062 ± 0.002	0.33	0.19 ± 0.04	0.0034 ± 0.0006	300 ± 140	1
-2G/C	0.75 ± 0.01	0.013 ± 0.0002	0.026 ± 0.002	0.50	0.146 ± 0.002	0.00257 ± 0.00004	25 ± 1.7	10
-2C/G	0.68 ± 0.03	0.012 ± 0.001	0.031 ± 0.004	0.39				

of dATP (0.005-1 μM) in 10 mM $MgCl_2$, were loaded into separate 18 μL loops of the RQF3 quench flow apparatus. Enzyme catalysis was initiated by rapidly mixing solutions A and B together followed by quenching with 100 mM EDTA at reaction times ranging from 10 ms to 60 sec at 37°C. Primer extensions were analyzed by 20% PAGE and the intensities of the gel bands were quantified by PhosphorImager analysis. Data were then plotted using the appropriate rate equations as previously described (*26*). Time course data for fixed nucleotide concentrations were fitted to Equation 1 by nonlinear regression analysis. In this expression, A is the amplitude of the burst phase, k_{obs} is the rate constant of the burst phase at the given [dATP], and k_{ss} is the steady state rate constant. Values of k_{obs} were graphed as a function of [dATP] using Equation 2 to obtain k_{pol}, the maximum rate constant of the pre-steady state burst phase and K_d^{dATP}, the dissociation constant of the nucleotide triphosphate from the HIV-1 RT•T/P complex.

Equation 1.

$$[product] = A\,(1\text{-}e^{k_{obs}t}) + k_{ss}t$$

Equation 2.

$$k_{obs} = \frac{k_{pol}\,[dATP]}{k_d^{dNTP} + [dATP]}$$

Active site titration

Active site titrations were carried out using varying concentrations of T/P under conditions of fixed HIV-1 RT concentration and saturating dNTP (*26*). Solution A, consisting of HIV-1 RT (37 nM) and T/P concentrations ranging from 12.5-200 nM in 50 mM Tris-HCl/NaCl (pH 7.5) were rapidly mixed with solution B (100 μM dATP and 10 mM $MgCl_2$) and reacted over times ranging from 5 msec to 30 sec in the RQF3 apparatus at 37°C. Primer extensions were analyzed and quantified as described above. Burst amplitudes were obtained from plots of product formation as a function of time for individual T/P concentrations. The dependence of the burst amplitudes as a function of [T/P] was then fitted to Equation 3 by nonlinear regression analysis. K_D is the dissociation constant for the HIV-1 RT•T/P complex and [E] is the concentration of active HIV-1 RT molecules.

Equation 3.

$$A = 0.5(K_D + [E] + [T/P]) - \sqrt{0.25(K_D + [E] + [T/P])^2 - [E][T/P]}$$

RNase H cleavage assay

100 nM T/P containing 0.1 μCi [γ-^{32}P]5'-labeled RNA template was incubated with 37 nM of HIV-1 RT in 50 mM Tris-HCl/NaCl (pH 7.5) at 37°C. Reactions were initiated by the addition of 5 mM $MgCl_2$. Aliquots (10 μL) were removed at time points between 0.25-20 min and quenched as described for steady state analyses. Fragmentation was analyzed by electrophoresis and quantified as described above. The rate of RNA cleavage was determined by fitting the data to a single-exponential decay equation.

Heteroduplex melting analyses

UV melting isotherms were measured on an Ultraspec 3000 *pro* equipped with a Peltier thermoelectric unit. Data were acquired using SWIFT-Tm software (Amersham Pharmacia Biotech). Equimolar concentrations of RNA template and DNA primer over a range of 0.5-3.0 mM were heated to 95°C for 10 min and then slowly annealed to 35°C in 50 mM Tris-HCl/NaCl, pH 7.5 prior to initiating melting at a rate of 0.5°C/min. Melting was monitored by absorbance at 260 nm over a temperature range of 35-70°C. Thermodynamic parameters were derived from plots of T_m^{-1} *vs.* ln [T/P]. ΔH was determined by fitting to the van't Hoff equation (Equation 4) where T_m is the melting temperature, [T/P] is the heteroduplex concentration, and R is the universal gas constant (1.987 cal•K^{-1} mol^{-1}).

Equation 4.

$$\frac{1}{T_m} = \frac{R}{\Delta H}\ln\frac{[T/P]}{4} + \frac{\Delta S}{\Delta H}$$

Results

Steady state kinetic analysis

Steady-state kinetic parameters were determined for the incorporation of dATP and dGTP opposite three contiguous uracil residues (U970-972) of an RNA template derived from the *env* gene of HIV-1 strain WMJ1. The effects of single base pair changes in the T/P stem on polymerase kinetics were determined. The WMJ1 control T/P and uniquely-substituted variants used in this study are shown in Figure 1. Steady state data for WMJ1, -2 and -6 substituted T/Ps are compiled in Table 1. The apparent second order rate constants ($k_{2app} = k_{cat}/K_M$) were used to evaluate the influence of upstream sequences on the relative efficiency of dATP or dGTP incorporation.

The observed k_{2app} value for the incorporation of dATP on the control WMJ1 template was 0.3 $s^{-1}\mu M^{-1}$. All possible single basepair substitutions at the -2 position did not greatly affect this value. Replacement of the A/T basepair at this position with U/A or C/G yielded nearly identical numbers, while replacement with G/C resulted in a less than 2-fold change. However substitution of the WMJ1 C/G pair at the -6 position with A/T resulted in a 14-fold increase in k_{2app} for dATP incorporation. Replacement with U/A at the -6 position had no effect on the incorporation efficiency of dATP, while replacement with G/C resulted in a 2-fold increase.

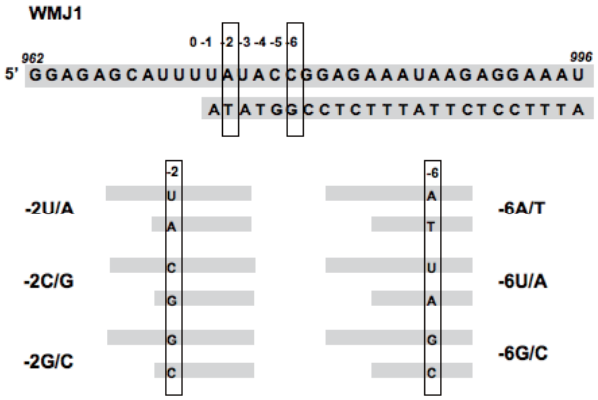

Figure 1. Template/primer (T/P) substrates used to measure the kinetic effects of sequence variation on HIV-1 RT catalyzed dNTP incorporation and RNase H activity. The control sequence corresponds to nucleotides 962-996 of the *env* gene of HIV strain WMJ1. Single basepair substitutions were made at either the -2 or -6 nucleotide positions, denoted by rectangles.

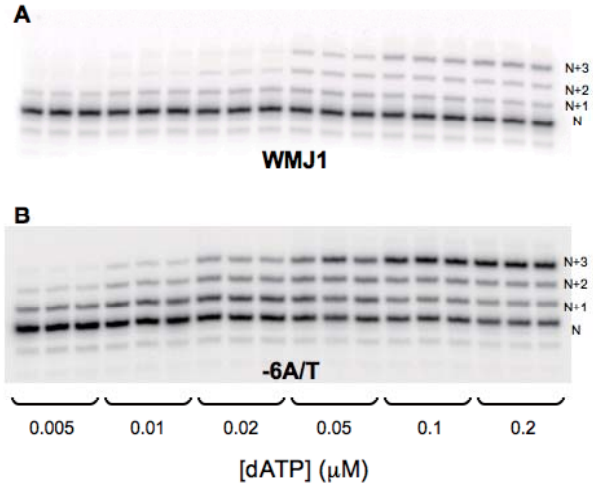

Figure 2. Primer extension data for dATP incorporation opposite U by HIV-1 RT on WMJ1 control and -6A/T substituted T/Ps. Enzyme and T/P concentrations were 50 and 150 nM, respectively. (A) Data acquired using WMJ1 (-6C/G), and (B) -6A/T substituted templates.

The relatively large increase in incorporation efficiency as a result of -6A/T substitution was readily observable from the primary gel electrophoresis data. Figures 2A and B present results for polymerization reactions with dATP conducted under identical conditions for control and -6A/T substituted T/Ps, respectively. Extension of primers of length N on WMJ1 control templates to yield products of length N+3 were observed between 20 and 50 nM dATP. Substitution with -6A/T lowered the concentration of dATP required for extension to between 5 and 10 nM. An increase in the efficiency of dGTP incorporation opposite U relative to control was similarly observed upon -6A/T substitution. This single base change resulted in a 7-fold increase in k_{2app} for U/G mispair formation. Product corresponding to formation of three successive U/G mispairs could not be observed in primer extension reactions using control template for dGTP concentrations up to 0.8 mM, but was readily detected in the -6A/T substituted T/P at 0.4 mM (data not shown). Smaller increases (~3-fold) in mispair formation were observed upon substitution of a G/C basepair at either the -2 or -6 positions. Substitution with U/A at the -2 or -6 position in the control template decreased the efficiency of U/G mispair formation by 4- and 3-fold, respectively.

The influence of both K_M and k_{cat} on the dNTP incorporation efficiency can be ascertained from Table 1. For example, the 14-fold increase in k_{2app} for U/A basepair formation resulting from A/T substitution at the -6 position reflects a 7-fold decrease in K_M and a 2-fold increase in k_{cat}. This same substitution influences the mispairing reaction with dGTP by lowering K_M 4-fold and similarly increasing k_{cat} by 2-fold. Although k_{cat} values obtained from the Michaelis-Menten approximation applied to polymerase reactions are normally considered to reflect rate limiting product release, a mechanistic interpretation of K_M is usually not possible. In order to obtain more detailed kinetic information on how the T/P sequence composition influences the various steps of the polymerization reaction, pre-steady state analyses were carried out using chemical quench flow methods (*26*) for WMJ1 and the -6A/T substituted T/Ps.

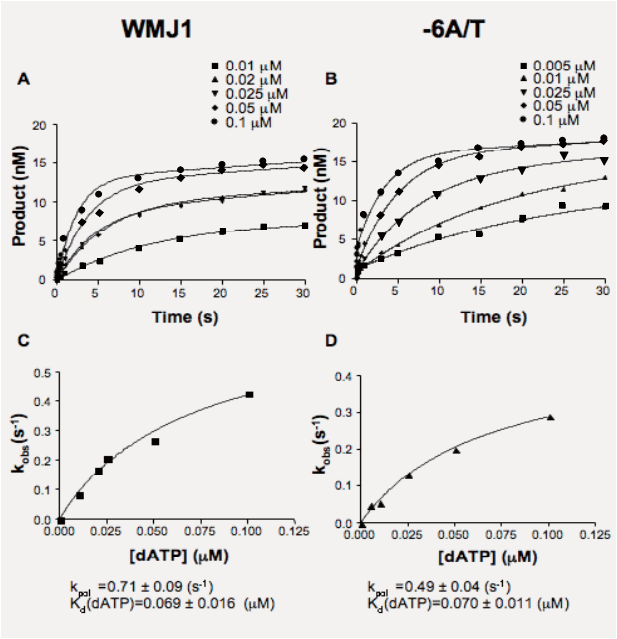

Figure 3. Pre-steady state kinetic analysis of U/A basepair formation. Product formation as a function of time was measured by the rapid quench flow technique using a KinTek RQF3 apparatus. Data were fitted to the single exponential of Equation 1 as described in Materials and Methods to obtain the curves shown in (A) for WMJ1 and (B) for -6A/T substituted T/Ps at the indicated dATP concentrations. Rate constants obtained in (A) and (B) were then graphed as a function of dATP concentration using Equation 2 in order to obtain values for k_{pol} and K_d^{dATP} for WMJ1 (C) and -6A/T (D) T/Ps.

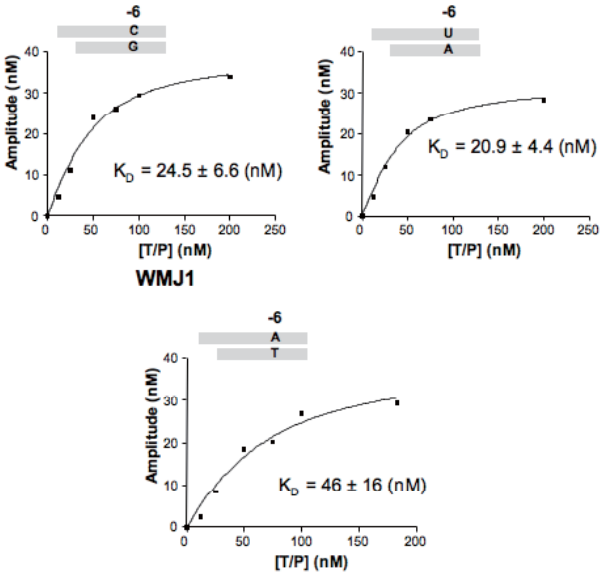

Figure 4. Determination of K_D for binding of HIV-1 RT to (A) WMJ1, (B) -6U/A, and (C) -6A/T T/Ps. Plots of product formation as a function of time for T/P concentrations ranging from 12.5-200 nM were initially obtained using conditions of saturating dATP (50 μM) and 30 nM HIV-1 RT. Plots of burst amplitudes as a function of T/P concentration were then constructed by fitting to Equation 3 to obtain K_D values.

Pre-steady state kinetics

Figures 3A, B show the pre-steady state kinetic data for product formation using the WMJ1 and -6A/T substituted T/Ps. Time course plots of product formation as a function of dATP concentration were obtained by fitting to Equation 1. The concentration dependence of the burst amplitudes (k_{obs}) was then fitted to Equation 2 to obtain K_d, the equilibrium dissociation constant for binding of dATP to the HIV-1 RT•T/P complex, and k_{pol}, the rate of phosphodiester bond formation. These results are shown in Figures 3C, D for the control and -6A/T T/Ps, respectively. The values of K_d obtained for control and -6A/T T/Ps were identical, indicating that the increases in incorporation efficiency resulting from -6A/T substitution were not due to increased polymerase binding of dATP. The values for k_{pol} were 0.71 ± 0.09 s^{-1} for control and 0.49 ± 0.04 s^{-1} for -6A/T T/Ps. The similarity of these values suggested that the rate of phosphodiester bond formation was not markedly influenced by T/P base composition at the -6 position.

Active site titrations were carried out by varying the concentrations of T/P (12.5-200 nM) for a fixed amount of HIV-1 RT at saturating dATP in order to establish the value of K_D (k_{off}/k_{on}) for initial enzyme binding to the RNA/DNA heteroduplexes. K_D values were determined for control, -6A/T and -6U/A substituted T/Ps. The latter T/P yielded the same k_{2app} value for U/A basepair formation as the control (Table 1), and hence served as an additional probe for examining the influence of K_D on incorporation efficiency. Burst amplitudes of product formation for different concentrations of T/P were initially determined (data not shown). These data were then fitted to Equation 3 in order to obtain values for K_D as shown in Figures 4A-C. Values for K_D were the same within experimental error for the control (-6C/G) and -6U/A T/Ps (~20 nM). However the value for the -6A/T substituted T/P was significantly larger, ~50 nM. Since the burst amplitudes directly reflect the concentration of active polymerase, comparison of these values with the protein concentration determined from spectrophotometric or Bradford assays provides an estimate of the percent of functional enzyme. These calculations typically indicated 50-60% polymerase activity.

RNase H cleavage

The RNase H activity associated with HIV-RT plays a critical role in the removal of the RNA template during 1st strand DNA synthesis (*27*). The effect of T/P sequence context on the RNase H activity was examined by measuring the rate of disappearance of 5'-end labeled RNA template under conditions of catalytic RT in the absence of dNTPs. The time course for hydrolysis of variously substituted T/Ps is shown in Figure 5. Rate constants for RNA cleavage were determined by fitting to a single exponential and are shown in the inset. The substitution of -6A/T was

observed to slow the rate of RNA cleavage by ~3-fold relative to the control sequence, whereas all other substitutions at either the -2 or -6 positions did not affect the relative cleavage rate.

T/P thermodynamic stability

In order to determine whether a relationship might exist between T/P sequence composition, thermodynamic stability, and polymerase incorporation efficiency, enthalpies (ΔH) associated with melting were determined for WMJ1, -6A/T and -6U/A templates. Van't Hoff plots obtained from optical melting data are shown in Figure 6. The WMJ1 control T/P with a C/G basepair at the -6 position was found to be the most stable, characterized by ΔH = -129 kcal/mol. Single substitutions with -6A/T or -6U/A basepairs lowered this value to -99 and -86 kcal/mol respectively. In spite of the 43 kcal/mol difference observed for -6U/A and control T/Ps, the apparent second order rate constants for dATP incorporation were identical (Table 1).

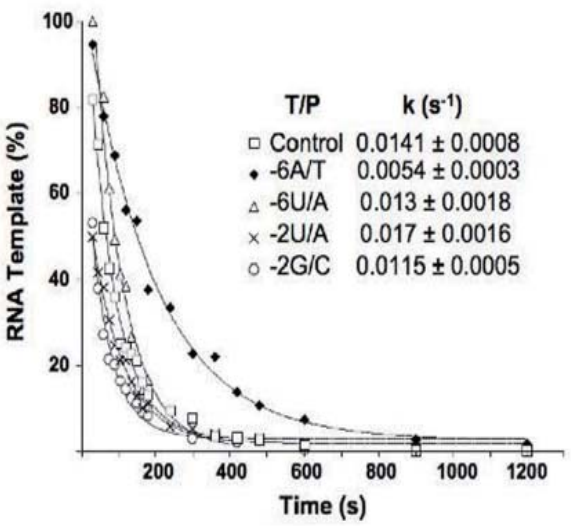

Figure 5. The influence of T/P base substitutions on the HIV-1 RT associated RNase H activity. The rate of disappearance of 5'-end labeled RNA within the heteroduplex T/P was determined by fitting integrated gel-electrophoresis data to a single exponential. Rate constants (average of 3 determinations) are shown in the inset.

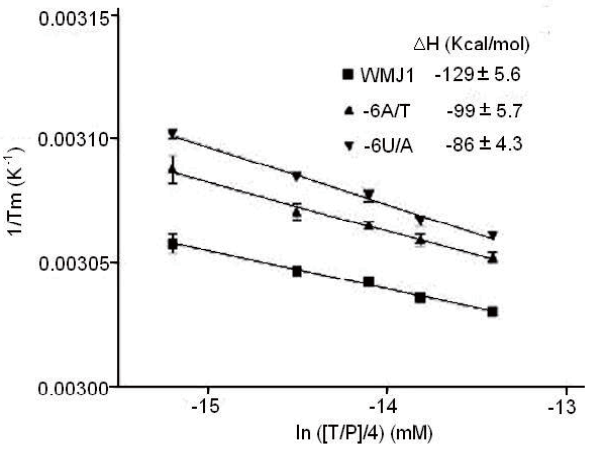

Figure 6. Enthalpies of melting for WMJ1 (-6C/G), -6A/T and -6U/A T/Ps. Values for ΔH were determined from plots of T_m^{-1} *vs.* ln ([T/P]/4) using the van't Hoff equation (Equation 4).

Discussion

In this work we have attempted to provide a mechanistic rationale for how certain sequence contexts may modify the activity of polymerases such as HIV-1 RT and influence fidelity. We have shown that a specific base substitution within an *env*-derived T/P sequence can exert a nearly 10-fold effect on polymerase incorporation efficiency even when situated remotely from the dNTP incorporation site. In contrast, 6 other T/P base substitutions examined exerted either small (≤ 3 fold) or negligible effects on the polymerase and RNase H activities. Base substitutions within the T/P likely regulate nucleotide incorporation efficiency by modulating non-covalent interactions with HIV-1 RT during one or more of the reaction steps. A simplified polymerase reaction mechanism which omits the conformational changes required for activated complex formation (*28,29*) is shown in Scheme 1. Several plausible models for how sequence context might regulate RT activity were considered within the context of this mechanistic scheme, known crystallographic information and the results of our steady and pre-steady state kinetic data.

One mechanism which could account for the observed sequence context effects on polymerase activity involves basepair recognition by RT amino acid side chains via the major or minor groove of the T/P. However, structures deduced from crystallographic data of HIV-1 RT•T/P complexes reveal very few direct basepair/amino acid interactions. Structures obtained at ~3Å resolution for HIV-1 RT complexes with either RNA/DNA or DNA/DNA T/Ps indicate that the majority of amino acid side chains interact with the primer or template ribophosphate backbone (*18-20*). Specific binding interactions between the T/P and HIV-1 RT appear to be highly conserved since nearly identical points of contact have been described for complexes with different T/P sequences (*18-20*). These are shown

$$E+T/P_n \underset{k_{off}}{\overset{k_{on}}{\rightleftharpoons}} E\text{-}T/P_n \overset{dNTP}{\underset{k_D}{\rightleftharpoons}} E\text{-}T/P_n\text{-}dNTP \overset{k_{pol}}{\underset{PPi}{\rightleftharpoons}} E\text{-}T/P_{n+1} \overset{k_{cat}}{\rightleftharpoons} E+T/P_{n+1}$$

Scheme 1. A simplified mechanism for primer elongation catalyzed by HIV-1 RT.

in Figure 7 for a sequence corresponding to the -6A/T substituted T/P. These structural considerations are not consistent with a mechanism involving a direct "readout" of the base composition.

Perturbations in van der Waals and hydrogen bonding interactions induced by local changes in helix geometry as a result of specific basepair substitutions may be relayed to the polymerase active site via conformational changes in the polypeptide backbone. In this mechanism, enhancement or inhibition of catalytic efficiency could occur as a result of a slight spatial rearrangement of the polymerase active site. This might be expected to result in variations in either the dNTP binding affinity (K_d) and/or in k_{pol}, the rate of phosphodiester bond formation (*30*). However, pre-steady state kinetics did not reveal any variations in these parameters as a result of -6A/T substitution. Sequence dependent variation in T/P thermodynamic stability could in principle influence the kinetics of dNTP incorporation by modifying interactions with the polymerase. However, no relationship was observed between melting enthalpies and apparent second order rate constants. Identical k_{2app} values for dATP incorporation were observed for T/Ps with widely divergent ΔH values (ΔΔH ~40 kcal/mol), suggesting that T/P thermodynamic stability does not influence the polymerase function of HIV-1 RT.

Alternatively, nucleotide sequence composition may modify polymerization kinetics by controlling the binding and dissociation of RT to the T/P. In order to determine whether base substitutions at the critical -6 position could modulate K_D (k_{off}/k_{on}) for initial polymerase binding (Scheme 1), active site titrations were carried out for the control WMJ1 (-6C/G), -6U/A and -6A/T T/Ps. The K_D values for the wild type and -6U/A T/Ps were nearly identical; however, a more than 2-fold increase was observed upon replacement with A/T at the -6 position. Increases in K_D result in a decrease in polymerase processivity, requiring multiple cycles of RT binding and dissociation in order to effect primer extension (*26*). Since only a fraction of HIV-1 RT molecules possess polymerase activity, increasing the T/P encounter frequency elevates the probability that productive reactions will occur. This results in enhanced incorporation efficiency. Product release by polymerases is typically the rate-limiting (slowest) step in the reaction sequence, and is directly reflected in the steady state k_{cat} values. Additional evidence that the -6A/T substitution influenced RT binding interactions was provided by the fact that the values of k_{cat} for both correct and incorrect basepair formation were increased to the same extent (2 fold) relative to the control WMJ1 sequence (Table 1). No other basepair substitution examined in this study was observed to increase k_{cat} relative to the control T/P. Thus perturbation of RT binding interactions both prior to and subsequent to the dNTP incorporation step by a specific basepair change can influence polymerization efficiency.

In order to further examine the effects of sequence composition on the enzymatic functions of RT, RNA hydrolysis by the RT associated RNase H activity was measured for different T/P substrates. RNase H cleavage of the template strand was monitored in the absence of dNTPs in order to uncouple RT catalyzed RNA hydrolysis from the polymerization reaction. Results of these experiments (Figure 5) revealed little variation in the extent of RNA hydrolysis among the tested substrates except for the -6A/T substituted T/P, which was cleaved at a 3-fold lower rate. Since the RNase H active site of RT is located 18-19 nucleotides from the primer terminus (*8,20,31,32*), it is unlikely that the -6A/T substitution directly inhibits the hydrolysis reaction. Reduction in RNase H activity is likely due to enhanced dissociation of RT from the T/P, a conclusion which is consistent with the increase in K_D determined from the pre-steady state experiments.

The earlier work of Abbotts *et al*. demonstrated enhanced termination probabilities for HIV-1 RT catalyzed primer extensions at sites 2 and 6 nt downstream from template adenines in an M13mp2 DNA template (*7*). These observations are partly in agreement with our results for -6 A/T substitutions on RNA templates, although adenine substitutions at the -2 position did not have as large an impact. The enhanced termination frequencies reported for the M13mp2 DNA template and our data obtained using RNA templates suggest that modulation of RT efficiency by a substitution at the -6 position may be operative for both RNA and DNA templates of unrelated sequence. Crystallographic studies suggest that the -6T/P local environment interacts in a unique manner with HIV-1 RT. Reverse transcriptase binding induces a bend of ~41º extending over the -5 to -9 positions, inducing an A to B form helical transition (*18,20,33*). The axis of curvature is most acute between the basepair step corresponding to positions -6 and -7, which forms the junction region between A and B forms. This may allow especially close approach of amino acid side chains of the αH and αK helices to the -6 basepair environment. Comparison of the amino acid side chains in contact with the -2 and -6 basepair regions reveals a significantly higher local concentration of basic and amide containing residues at the latter position. These differences are highlighted in the 3 dimensional representation shown in Figure 8, based on the crystal structure of HIV-1 RT bound to an RNA/DNA T/P (*20*). Many of these amino acids are involved in potential hydrogen bonds with the ribophosphate backbone of both the primer and template strands. Residues N255, Q258 and N265 reside in helix αH, while K353 and K374 are localized within β18 and helix αK, respectively. In contrast, the majority of polymerase contacts to the -2T/P basepair consist predominantly of acidic and neutral side chains (with the exception of

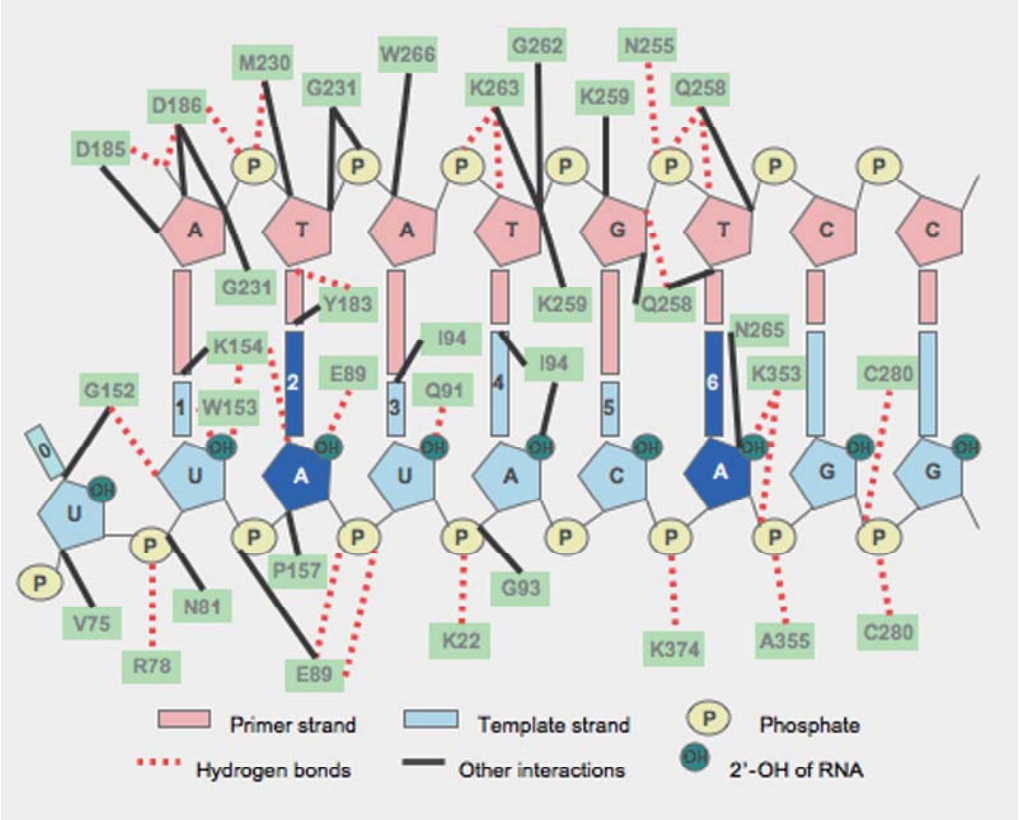

Figure 7. Schematic of non-covalent interactions observed between heteroduplex T/Ps and amino acid side chains of HIV-1 RT based on the crystal structure of Sarafianos *et al*. (reference 20).

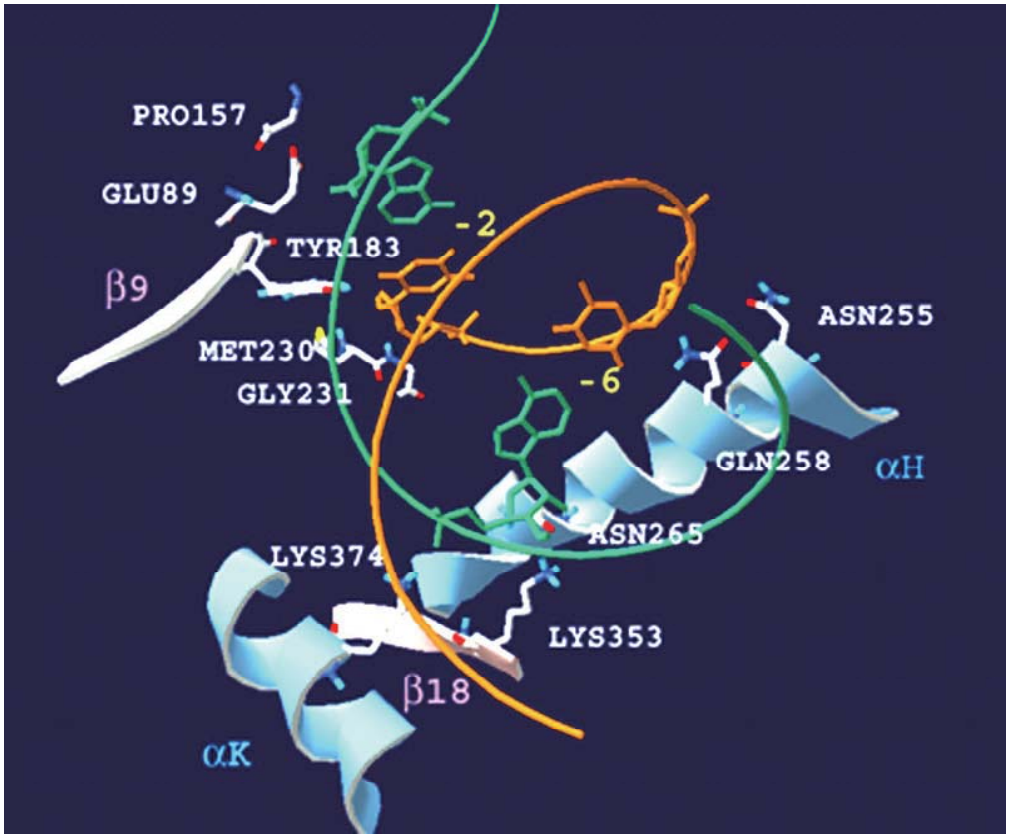

Figure 8. 3-D representation of the complex between HIV-1 RT and T/P substrate emphasizing the -2 and -6 basepair environments. The template RNA and DNA primer strands are shown in green and orange respectively. An increased density of basic and amide containing side chains can be observed at the -6 basepair. Image was constructed from protein data bank file IHYS using the Deep View Swiss – PDB viewer.

K154). We suggest that -6A/T substitution results in a local conformational change which leads to partial destabilization of some of these highly polar non-covalent interactions with the ribophosphate backbone, which in turn influences the binding and dissociation of HIV-1 RT. A modest decrease in hydrogen bonding distance of only ~0.5Å would result in a significant decrease in stabilization energy (*34*). The observed changes in k_{2app} values can be used to calculate the effects of T/P substitutions on HIV-1 RT mismatch frequency. The frequency of mismatch formation is defined by the reciprocal insertion frequency, $1/f_{ins}$, defined by Goodman and coworkers as the ratio $k_{2app}^{correct}/k_{2app}^{incorrect}$ (*35*). Using the values in Table 1, formation of a U/G mismatch at position 973 of the *env* gene of HIV strain WMJ1 would be observed once in 10,000 replication events. Substitution of A/T at the -6 position would lower this frequency to 1 in 20,000, resulting in a 2-fold increase in polymerase fidelity.

The effects of T/P basepair substitutions on the apparent second order rate constants were more variable for the mispairing reaction than for U/A basepair formation (Table 1). For example, -6U/A and -2U/A substitutions lowered k_{2app} for U/G mispairs by ~4 and 3-fold, respectively. In contrast, the -6G/C and -2G/C substitutions increased k_{2app} for this mispair by ~3-fold. These were the only base substitutions examined which would decrease RT fidelity. It is not clear why the apparent second order rate constants for the U/G mispairing reaction were more sensitive to T/P basepair substitutions. Perhaps in the absence of the greater kinetic and thermodynamic stabilization afforded by Watson-Crick base pairing, the energetically disfavored process of mismatch formation becomes more influenced by small perturbations in RT-T/P interactions resulting from sequence variation. However, even for the U/G mismatch, the largest effect on k_{2app} (7 fold change) was observed for the -6A/T substitution. It is not possible to assess the generality of the specific sequence context effect observed in this study, since only a small sample of sequence space can be feasibly probed using kinetic methods. However, we suggest that K_D modulation by specific base substitutions may constitute one mechanism whereby basepair composition can influence the fidelity of RT and other polymerases for certain sequence contexts.

Acknowledgements

We would like to thank Dr. Gerald E. Wuenschell for helpful comments and discussions, and Hong Zang and Prof. F. P. Guengerich of Vanderbilt University for help with the purification of HIV-1 RT.

This work was supported by PHS grant GM53962 to J.T.

References

1. Roberts JD, Bebenek K, Kunkel TA. The accuracy of reverse transcriptase from HIV-1. Science 1988;242:1171-1173.
2. Ji J, Loeb LA. Fidelity of HIV-1 reverse transcriptase copying a hypervariable region of the HIV-1 *env* gene. Virology 1994;199:323-330.
3. Preston BD, Poiesz BJ, Loeb LA. Fidelity of HIV-1 reverse transcriptase. Science 1988;242:1168-1171.
4. Mansky LM, Temin HM. Lower *in vivo* mutation rate of human immunodeficiency virus type 1 than that predicted from the fidelity of purified reverse transcriptase. J Virol 1995;69:5087-5094.
5. Perelson AS, Neumann AU, Markowitz M, Leonard JM, Ho DD. HIV-1 dynamics *in vivo*: virion clearance rate, infected cell life-span, and viral generation time. Science 1996;271:1582-1586.
6. Bebenek K, Abbotts J, Wilson SH, Kunkel TA. Error-prone polymerization by HIV-1 reverse transcriptase. Contribution of template-primer misalignment, miscoding, and termination probability to mutational hot spots. J Biol Chem 1993;268:10324-10334.
7. Abbotts J, Bebenek K, Kunkel TA, Wilson SH. Mechanism of HIV-1 reverse transcriptase. Termination of processive synthesis on a natural DNA template is influenced by the sequence of the template-primer stem. J Biol Chem 1993;268:10312-10323.
8. Suo Z, Johnson KA. Effect of RNA secondary structure on the kinetics of DNA synthesis catalyzed by HIV-1 reverse transcriptase. Biochemistry 1997;36:12459-12467.
9. Suo Z, Johnson KA. RNA secondary structure switching during DNA synthesis catalyzed by HIV-1 reverse transcriptase. Biochemistry 1997;36:14778-14785.
10. Ji X, Klarmann GJ, Preston BD. Effect of human immunodeficiency virus type 1 (HIV-1) nucleocapsid protein on HIV-1 reverse transcriptase activity *in vitro*. Biochemistry 1996;35:132-143.
11. Wu W, Henderson LE, Copeland TD, Gorelick RJ, Bosche WJ, Rein A, Levin JG. Human immunodeficiency virus type 1 nucleocapsid protein reduces reverse transcriptase pausing at a secondary structure near the murine leukemia virus polypurine tract. J Virol 1996;70:7132-7142.
12. Lapadat-Tapolsky M, Gabus C, Rau M, Darlix JL. Possible roles of HIV-1 nucleocapsid protein in the specificity of proviral DNA synthesis and in its variability. J Mol Biol 1997;268:250-260.
13. Jaruga P, Jaruga B, Olczak A, Halota W, Olinski R. Oxidative DNA base damage in lymphocytes of HIV-infected drug users. Free Radic Res 1999;31:197-200.
14. Valentine MR, Termini J. Kinetics of formation of hypoxanthine containing base pairs by HIV-RT: RNA template effects on the base substitution frequencies. Nucleic Acids Res 2001;29:1191-1199.
15. Wuenschell GE, Valentine MR, Termini J. Incorporation of oxidatively modified 2'-deoxynucleotide triphosphates by HIV-1 RT on RNA and DNA templates. Chem Res Toxicol 2002;15:654-661.
16. Klarmann GJ, Smith RA, Schinazi RF, North TW, Preston BD. Site-specific incorporation of nucleoside analogs by HIV-1 reverse transcriptase and the template grip mutant P157S. Template interactions influence substrate recognition at the polymerase active site. J Biol Chem 2000;275:359-366.
17. Boyer PL, Tantillo C, Jacobo-Molina A, Nanni RG, Ding J, Arnold E, Hughes SH. Sensitivity of wild-type human immunodeficiency virus type 1 reverse transcriptase to dideoxynucleotides depends on template length; the sensitivity of drug-resistant mutants does not. Proc Natl Acad Sci U S A 1994;91:4882-4886.
18. Ding J, Hughes SH, Arnold E. Protein-nucleic acid

interactions and DNA conformation in a complex of human immunodeficiency virus type 1 reverse transcriptase with a double-stranded DNA template-primer. Biopolymers 1997;44:125-138.
19. Huang H, Chopra R, Verdine GL, Harrison SC. Structure of a covalently trapped catalytic complex of HIV-1 reverse transcriptase: implications for drug resistance. Science 1998;282:1669-1675.
20. Sarafianos SG, Das K, Tantillo C, Clark AD, Jr. Ding J, Whitcomb JM, Boyer PL, Hughes SH, Arnold E. Crystal structure of HIV-1 reverse transcriptase in complex with a polypurine tract RNA:DNA. Embo J 2001;20:1449-1461.
21. Beard WA, Bebenek K, Darden TA, Li L, Prasad R, Kunkel TA, Wilson SH. Vertical-scanning mutagenesis of a critical tryptophan in the minor groove binding track of HIV-1 reverse transcriptase. Molecular nature of polymerase-nucleic acid interactions. J Biol Chem 1998;273:30435-30442.
22. Bebenek K, Beard WA, Darden TA, Li L, Prasad R, Luton BA, Gorenstein DG, Wilson SH, Kunkel TA. A minor groove binding track in reverse transcriptase. Nat Struct Biol 1997;4:194-197.
23. Sevilya Z, Loya S, Duvshani A, Adir N, Hizi A. Mutagenesis of cysteine 280 of the reverse transcriptase of human immunodeficiency virus type-1: the effects on the ribonuclease H activity. J Mol Biol 2003;327:19-30.
24. Starcich BR, Hahn BH, Shaw GM, McNeely PD, Modrow S, Wolf H, Parks ES, Parks WP, Josephs SF, Gallo RC, Wong-Staal F. Identification and characterization of conserved and variable regions in the envelope gene of HTLV-III/LAV, the retrovirus of AIDS. Cell 1986;45:637-648.
25. Borer PN. In Fassman GD. (ed.), Handbook of Biochemistry and Molecular Biology, 3rd Edition. CRC Press, Cleveland, OH, Vol. 1, pp. 589-595, 1975.
26. Johnson KA. Rapid quench kinetic analysis of polymerases, adenosinetriphosphatases, and enzyme intermediates. Methods Enzymol 1995;249:38-61.
27. Klarmann GJ, Hawkins ME, Le Grice SF. Uncovering the complexities of retroviral ribonuclease H reveals its potential as a therapeutic target. AIDS Rev 2002;4:183-194.
28. Kati WM, Johnson KA, Jerva LF, Anderson KS. Mechanism and fidelity of HIV reverse transcriptase. J Biol Chem 1992;267:25988-25997.
29. Hsieh JC, Zinnen S, Modrich P. Kinetic mechanism of the DNA-dependent DNA polymerase activity of human immunodeficiency virus reverse transcriptase. J Biol Chem 1993;268:24607-24613.
30. Weiss KK, Chen R, Skasko M, Reynolds HM, Lee K, Bambara RA, Mansky LM, Kim B. A role for dNTP binding of human immunodeficiency virus type 1 reverse transcriptase in viral mutagenesis. Biochemistry 2004;43:4490-4500.
31. Suo Z, Johnson KA. Effect of RNA secondary structure on RNA cleavage catalyzed by HIV-1 reverse transcriptase. Biochemistry 1997;36:12468-12476.
32. Gopalakrishnan V, Peliska JA, Benkovic SJ. Human immunodeficiency virus type 1 reverse transcriptase: spatial and temporal relationship between the polymerase and RNase H activities. Proc Natl Acad Sci U S A 1992;89:10763-10767.
33. Jacobo-Molina A, Ding J, Nanni RG, Clark Jr. AD, Lu X, Tantillo C, Williams RL, Kamer G, Ferris AL, Clark P, Hizi A, Hughesi SH, Arnold E. Crystal structure of human immunodeficiency virus type 1 reverse transcriptase complexed with double-stranded DNA at 3.0 A resolution shows bent DNA. Proc Natl Acad Sci U S A 1993;90:6320-6324.
34. Fersht AR. Catalysis, binding and enzyme-substrate complementarity. Proc R Soc Lond B Biol Sci 1974;187:397-407.
35. Boosalis MS, Petruska J, Goodman MF. DNA polymerase insertion fidelity. Gel assay for site-specific kinetics. J Biol Chem 1987;262:14689-14696.